PHYSICAL REVIEW B **79**, 140506(R) (2009)

^{59}Co and ^{75}As NMR investigation of lightly doped $Ba(Fe_{1-x}Co_x)_2As_2$ ($x=0.02,0.04$)

F. L. Ning,[1] K. Ahilan,[1] T. Imai,[1,2] A. S. Sefat,[3] R. Jin,[3] M. A. McGuire,[3] B. C. Sales,[3] and D. Mandrus[3]
[1]*Department of Physics and Astronomy, McMaster University, Hamilton, Ontario, Canada L8S4M1*
[2]*Canadian Institute for Advanced Research, Toronto, Ontario, Canada M5G1Z8*
[3]*Materials Science and Technology Division, Oak Ridge National Laboratory, Tennessee 37831, USA*
(Received 10 February 2009; revised manuscript received 20 March 2009; published 23 April 2009)

We investigate the electronic properties of $Ba(Fe_{1-x}Co_x)_2As_2$ ($x=0.02,0.04$) in the lightly electron-doped regime by ^{59}Co and ^{75}As NMR. We demonstrate that Co doping significantly suppresses the magnetic ordering temperature to the SDW state, T_{SDW}. Furthermore, ordered moments below T_{SDW} exhibit large distribution. Strong spin fluctuations remain even below T_{SDW}, persisting all the way down to 4.2 K. We find no signature of additional freezing of spin degrees of freedom unlike the case of the lightly hole-doped stripe phase of the cuprates.

DOI: 10.1103/PhysRevB.79.140506 PACS number(s): 74.70.−b, 76.60.−k

The recent discovery of high transition temperature (high-T_c) superconductivity in iron pnictides[1–4] has spurred huge excitement in the condensed-matter physics community. The FeAs layers, consisting of a square lattice of Fe coordinated by four As, are the crucial component responsible for the superconductivity. The quasi-two-dimensional layered structure is reminiscent of the CuO_2 layers in the high-T_c cuprates, but many dissimilarities exist between iron pnictides and cuprates. For example, doping ~4% of impurities into cuprates could destroy their superconductivity,[5] but doping Co or Ni into the FeAs layers of $BaFe_2As_2$ *induces* superconductivity with T_c as high as 22 K.[4,6] Earlier studies showed that a prototypical parent compound of iron pnictides, $BaFe_2As_2$($x=0$), is an itinerant antiferromagnet and exhibits simultaneous first-order structural and magnetic phase transitions at $T_{SDW}\sim 135$ K.[7–10] 2% and 4% Co doping into $BaFe_2As_2$ quickly suppresses the ordering temperatures to $T_{SDW}\sim 100$ K and 66 K, respectively.[11–15] When the doping level is increased to ~8%, superconductivity appears with optimized $T_c\sim 22$ K. Very little is known about the nature of the magnetically ordered state below T_{SDW} in the presence of 2%–4% electron doping.

In this Rapid Communication, we will report a microscopic investigation by nuclear magnetic resonance (NMR) on the electronic properties of lightly electron-doped $Ba(Fe_{1-x}Co_x)_2As_2$ ($x=0.02,0.04$). We will show that Co doping suppresses the magnetic ordering temperature, T_{SDW}. Furthermore, as little as 2% Co doping transforms the nature of the ground state from the commensurate spin density wave (C-SDW) state observed in the undoped parent compound $BaFe_2As_2$ (Refs. 7–9) to a different state, most likely a highly disordered incommensurate spin density wave (IC-SDW) state. We will show that strong spin fluctuations remain below T_{SDW} all the way down to 4.2 K. There is no signature of additional freezing of spin degrees of freedom in contrast with the case of the lightly doped stripe phase of the cuprates.[16,17]

We grew the single crystals with $x=0$, 0.02, and 0.04 from FeAs flux[4] and determined the actual Co concentration by energy dispersive x-ray spectroscopy. These are the identical pieces that were used for our previous ^{75}As NMR study in the paramagnetic state.[12,18] We carried out NMR measurements using the standard pulsed NMR techniques on either one piece of crystal ($x=0,0.04$) or aligned crystals ($x=0.02$, two pieces) with total masses of ~2 to ~20 mg.

In Fig. 1, we present the typical field swept line shapes at a fixed frequency $f=43.503$ MHz for ^{75}As (nuclear spin $I=\frac{3}{2}$, $\gamma_n/2\pi=7.2919$ MHz/T) with external field B_{ext} applied either along the c axis ($B_{ext}//c$) or within the ab plane ($B_{ext}//ab$). The nuclear spin Hamiltonian can be expressed as a summation of the Zeeman and nuclear quadrupole interaction terms,

$$H=-\gamma_n h\mathbf{B}\cdot\mathbf{I}+\frac{h\nu_Q^c}{6}\left\{3I_z^2-I(I+1)+\frac{1}{2}\eta(I_+^2+I_-^2)\right\}, \quad (1)$$

where h is Planck's constant and I is the nuclear spin. **B** is the local field at the observed nuclear spin, and the summa-

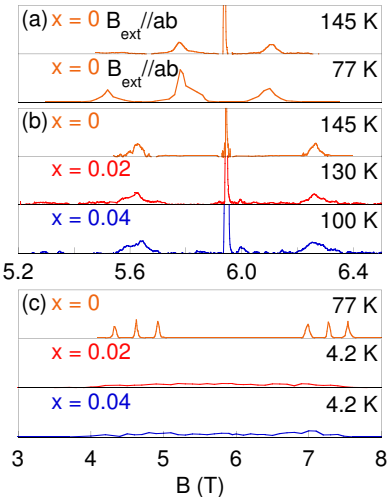

FIG. 1. (Color online) ^{75}As field swept NMR line shapes of $Ba(Fe_{1-x}Co_x)_2As_2$ measured at $f=43.503$ MHz, for $x=0(T_{SDW}=135$ K), $x=0.02(T_{SDW}=100$ K), and $x=0.04(T_{SDW}=66$ K). B_{ext} was applied along the c axis, except in panel (a) where $B_{ext}//ab$. Notice that the positions of the NMR lines in the paramagnetic state only shift from 145 to 77 K in (a) because the hyperfine magnetic field is along the c axis. In (c), NMR lines either split ($x=0$) or broaden ($x=0.02,0.04$).

tion of the external field $\mathbf{B}_{ext}$ and the hyperfine field $\mathbf{B}_{hf}$ from the ordered moments. The nuclear quadrupole interaction ν_Q^c is proportional to the electric field gradient (EFG) at the observed As site, and η is the asymmetry parameter of the EFG, $\eta=|\nu_Q^a-\nu_Q^b|/\nu_Q^c$.

First, we briefly discuss the ^{75}As NMR results in undoped $BaFe_2As_2$ ($x=0$, $T_{SDW}=135$ K). Each ^{75}As site gives rise to three transitions from $I_z=\frac{2m+1}{2}$ to $\frac{2m-1}{2}$ (where $m=-1, 0, 1$) in the paramagnetic state, as shown in Figs. 1(a) and 1(b). The fact that we observe only one set of ^{75}As NMR signals above T_{SDW} is evidence that there is only one type of As site in the undoped parent compound. The satellite transitions ($m=-1, 1$) are somewhat broader than the central peak ($m=0$), but are still fairly sharp, implying that ν_Q^c has a well-defined value. From the split between the main peak and the satellite peaks in Fig. 1(a), $\Delta B\sim 0.162$ T, we estimate $^{75}\nu_Q^{ab}=^{75}\gamma_n\Delta B=1.188$ MHz. From the split in Fig. 1(b), we estimate $^{75}\nu_Q^c=2.3$ MHz. Thus $\eta\cong 0$ at 145 K for ^{75}As, as expected for the tetragonal symmetry. At 77 K, the ^{75}As NMR lines with $B_{ext}//c$ split into two sets as shown in Fig. 1(c). This is because the hyperfine field at ^{75}As site from the ordered moments, $\pm B_{hf}$, is along the c axis. For $B_{ext}//ab$, the ^{75}As line only shifts to the lower field side, because the resonance condition is satisfied as $^{75}\gamma_n\sqrt{B_{ext}^2+B_{hf}^2}=f$. These results confirm that the hyperfine field on the As site is along the c axis.[9,10] The relatively sharp peaks at 77 K in the ordered state indicate that the ordered moments are commensurate with the lattice and the hyperfine field has only two discrete values, e.g., $B_{hf}^c=\pm 1.32$ T at 77 K.[9]

In Fig. 1(b), we also show the influence of Co doping in the paramagnetic state above T_{SDW}. The line shapes for the doped samples are very similar to the undoped case, except that the satellite transitions become broader due to additional distribution of $^{75}\nu_Q^c$ caused by the disorder in the lattice environment. The magnitude of $^{75}\nu_Q^c\sim 2.3$ MHz is by a factor of ~ 5 smaller than the case of $LaFeAsO_{1-\delta}$ (Ref. 19). This is presumably because ^{75}As ions are surrounded by 2+ ions only (Fe^{2+} and Ba^{2+}) in the present case, while ^{75}As ions in $LaFeAsO_{1-\delta}$ have La^{3+} and O^{2-} ions nearby, in addition to Fe^{2+} ions; the charge disparity would enhance the EFG, hence $^{75}\nu_Q^c$ in $LaFeAsO_{1-\delta}$. We also note that $^{75}\nu_Q^c\sim 2.3$ MHz is nearly independent of the level of doping, and there is no evidence for correlation between $^{75}\nu_Q^c$ and T_c. This is in contrast with the case of in $LaFeAsO_{1-\delta}$ where T_c appears to have a strong correlation with the $^{75}\nu_Q^c$ (Ref. 19). On the other hand, we found that the line shapes are qualitatively different between undoped and doped samples below T_{SDW}, as shown in Fig. 1(c). Unexpectedly, the ^{75}As lines do not split in 2% and 4% Co-doped samples. Instead, the ^{75}As NMR lines broaden and become almost featureless. The spin echo signal could be detected everywhere between 4 and 7.5 T, which implies that $|B_{hf}^c|$ at ^{75}As sites is continuously distributed from 0 to $\lesssim 1.32$ T.

In Fig. 2, we present the typical field swept ^{59}Co (nuclear spin $I=\frac{7}{2}$, $\gamma_n/2\pi=10.054$ MHz/T) line shapes with $B_{ext}//c$ or $B_{ext}//ab$. Co is randomly doped into FeAs layers by replacing Fe. The probability for each Co to have four Fe at the nearest neighbor (n.n.) sites is 92.2% for $x=0.02$ and 84.9% for $x=0.04$, respectively. Thus the Co NMR line shape is

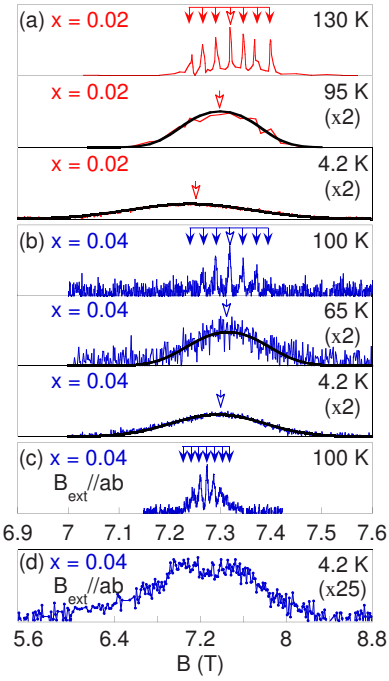

FIG. 2. (Color online) ^{59}Co field swept NMR line shapes of $Ba(Fe_{1-x}Co_x)_2As_2$ measured at $f=74.103$ MHz for (a) $x=0.02$ at 130 K (paramagnetic), 95 K, and 4.2 K (SDW); (b) $x=0.04$ at 100 K (paramagnetic), 65 K, and 4.2 K (SDW). The overall intensities in the SDW state have been amplified by a factor of 2 compared with those in the paramagnetic state. Solid curves represent Gaussian fit to the data. In (c) and (d), B_{ext} was applied within the ab plane, otherwise B_{ext} was applied along the c axis. Notice the scale of the horizontal axis in panel (d) is expanded. The overall intensity in (d) has been amplified by 25 times compared with (c). Open arrows mark where we measured T_1.

dominated by the NMR signals from the Co with four n.n. Fe, and the Co NMR line splits into seven peaks separated by $^{59}\nu_Q^c$. We estimate $^{59}\nu_Q^c\sim 0.26$ MHz, $^{59}\nu_Q^{ab}\sim 0.13$ MHz, and $\eta=0$ for both $x=0.02$ and 0.04.

Below T_{SDW}, the ^{59}Co NMR lines become broader and the seven discrete peaks caused by the quadrupole split $^{59}\nu_Q^c$ are smeared out. The whole NMR line becomes completely featureless at low temperatures. We observe no signature of residual sharp peaks below T_{SDW}, hence all ^{59}Co nuclear spins are under the influence of magnetic ordering. The integrated intensity corrected for the Boltzmann factor agrees well between 4.2 and 100 K, hence we observe all ^{59}Co nuclear spins at 4.2 K. This conservation of the total intensity rules out any possibility of phase separation or macroscopic inhomogeneity in the sample. Close inspection of the line positions reveals that the center of the broad line progressively shifts to the lower field side with decreasing temperature when we apply B_{ext} along the c axis. For example, the center transition for $x=0.04$ at 100 K is at $B_{ext}\sim 7.318$ T, which shifts by 0.023 T to 7.295 T at 4.2 K. On the other hand, the ^{59}Co NMR lines for $x=0.04$ split into two broad humps when B_{ext} is applied along the ab plane instead, as shown in Fig. 2(d). The separation between the center of the two broad humps, ~ 0.6 T, is much larger than the small shift, 0.023 T, observed along $B_{ext}//c$. This implies that the hyperfine field

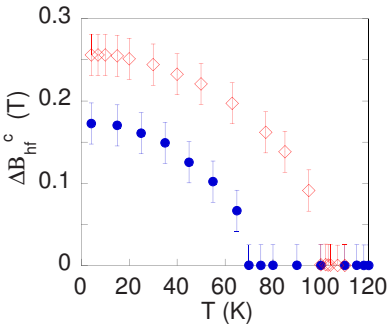

FIG. 3. (Color online) The temperature dependence of the magnetic broadening $\Delta B_{\mathrm{hf}}^{c}$ of ^{59}Co NMR lines for $x=0.02$ (◇) and $x=0.04$ (●).

at the ^{59}Co site is primarily within the *ab* plane. Combined with the fact that ^{75}As lines do not exhibit splitting with $B_{\mathrm{ext}}//c$, we conclude that Co doping changes the C-SDW spin structure of $BaFe_2As_2$.

We fit the broad, featureless ^{59}Co NMR line shapes with $B_{\mathrm{ext}}//c$ by assuming that the quadrupole splitting by $^{59}\nu_Q^c$ does not depend on temperature and all seven transitions become broader by a Gaussian distribution of the hyperfine fields $\Delta B_{\mathrm{hf}}^{c}$ below T_{SDW}. The fits are reasonable for both $x=0.02$ and 0.04, and we were able to deduce the Gaussian width $\Delta B_{\mathrm{hf}}^{c}$ as summarized in Fig. 3. $\Delta B_{\mathrm{hf}}^{c}$ continuously increases and finally saturates at base temperature.

In Fig. 4(a), we present the temperature dependence of the static spin susceptibility, χ, for $x=0.02$ and 0.04 as measured by ^{59}Co NMR Knight shift, K. We also plot the result for the superconducting $x=0.08$ sample for comparison.[18] In general, we can write $K=K_{\mathrm{spin}}+K_{\mathrm{chem}}$. K_{spin} is the spin contribution, which is proportional to the local spin susceptibility χ, while K_{chem} is the temperature-independent chemical shift. K_{chem} is not related to χ. Our results indicate that χ gradually

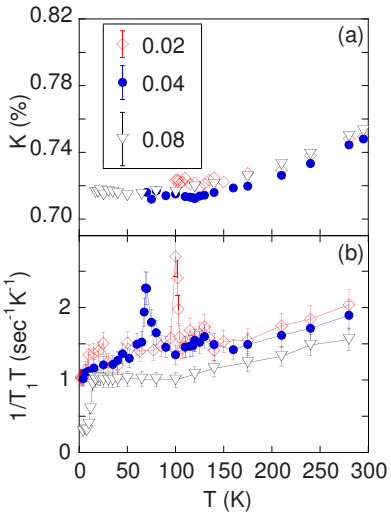

FIG. 4. (Color online) (a) ^{59}Co Knight shift for $x=0.02$ (◇), 0.04 (●), and 0.08 (▽). The error bars in the legend represent the full width at half maximum of Co center transition at 295 K. (b) $\frac{1}{T_1T}$ at ^{59}Co sites for $x=0.02$ (◇), 0.04 (●), and 0.08 (▽). We measured T_1 at the central transition, as shown by the open arrows in Fig. 2.

decreases below ~300 K and begins to level off below ~100 K. This is consistent with our earlier results based on ^{75}As NMR.[12] The ^{59}Co NMR linewidth is too broad to determine the concentration dependence accurately.

In Fig. 4(b), we show the temperature dependence of $\mathbf{q}$ integrated dynamical spin susceptibility as measured by $\frac{1}{T_1T}\propto\Sigma_{\mathbf{q}}|A_{\mathrm{hf}}(\mathbf{q})|^2\frac{\chi'(\mathbf{q},f)}{f}$ at ^{59}Co sites, where $|A_{\mathrm{hf}}(\mathbf{q})|^2$ is the wave-vector $\mathbf{q}$-dependent hyperfine form factor,[18] $\chi'(\mathbf{q},f)$ is the imaginary part of the dynamical electron spin susceptibility (i.e., spin fluctuations), and f is the NMR frequency ($\lesssim 10^2$ MHz). $\frac{1}{T_1T}$ shows a divergent behavior at ~100 K for $x=0.02$, and ~66 K for $x=0.04$. These temperatures agree well with the maximum negative slope observed for in-plane resistivity.[12] In Ref. 12, we also reported the divergent behavior of $^{75}(\frac{1}{T_1T})$ at ^{75}As sites with $B_{\mathrm{ext}}//c$ axis. In this geometry, $^{75}(\frac{1}{T_1T})$ probes spin fluctuations within the *ab* plane. On the other hand, Kitagawa *et al.*[9] showed that the ^{75}As hyperfine form factor satisfies $|^{75}A_{\mathrm{hf}}(\mathbf{q})|^2=0$ within the *ab* plane for commensurate spin fluctuations due to cancellation of the transferred hyperfine fields. Therefore, these $\frac{1}{T_1T}$ data at ^{59}Co and ^{75}As provide strong evidence for the critical slowing down of the incommensurate spin fluctuations toward a second-order phase transition at T_{SDW}. Interestingly, $\frac{1}{T_1T}$ decreases roughly linearly with temperature down to the base temperature for both $x=0.02$ and 0.04 except near T_{SDW}, and shows qualitatively the same behavior as that of the superconducting sample. Our results suggest that strong spin fluctuations remain even below T_{SDW} in Co-doped samples, which may be an indication that Fe 3*d* spins of some part of the 3*d* orbitals remain paramagnetic below T_{SDW} as suggested by Singh *et al.*[4,20] based on fermiology. For example, all 3*d* spins are not ordered in e_g but ordered in t_{2g} orbitals, or vice versa. In passing, we recall that $\frac{1}{T_1T}$ at ^{139}La sites in undoped LaFeAsO (Ref. 21) and ^{75}As sites in undoped $BaFe_2As_2$ (Refs. 9 and 10) is suppressed by an order of magnitude or more below T_{SDW}.

The large in-plane resistivity below T_{SDW} in Co-doped samples[11,12] is probably related to these strong spin fluctuations. It should also be noted that we find no signature of additional spin freezing at low temperatures in either $\frac{1}{T_1T}$ or $\Delta B_{\mathrm{hf}}^{c}$. It is worth recalling that in the case of lightly doped $La_{2-x}Sr_xCuO_2$,[16,17] $\frac{1}{T_1T}$ at ^{139}La sites shows additional diverging behavior at T_{sf}, much below T_N. Furthermore, B_{hf} shows additional enhancement below T_{sf}. The spin freezing temperature T_{sf} turned out to be related to glassy freezing of spin and charge stripes. Our present observation is markedly different from the case of the lightly doped cuprates.

In conclusion, we have presented a ^{59}Co and ^{75}As NMR study in the lightly electron-doped, SDW ordered regime of $Ba(Fe_{1-x}Co_x)_2As_2$. We demonstrated that Co doping suppresses T_{SDW}, and changes the spin structure. The continuous growth of the NMR linewidth below T_{SDW} and the strong enhancement of $\frac{1}{T_1T}$ at T_{SDW} suggest a second-order phase transition into an SDW phase, most likely incommensurate with the lattice and highly disordered. We did not detect any anomaly from T_{SDW} down to base temperature in either $\Delta B_{\mathrm{hf}}^{c}$ or $\frac{1}{T_1T}$. This suggests the absence of freezing of stripes or

other analogous phenomena. On the other hand, large $\frac{1}{T_1T}$ at $T \ll T_{SDW}$ hints the residual paramagnetic spins at *each* Fe site due to the multiorbital nature of FeAs layers. During the final stage of preparing this manuscript, Bernhard *et al.*[22] reported μSR observation of static magnetism in a 4% Co-doped sample only below 15 ~ 20 K.

The work at McMaster was supported by NSERC, CIFAR, and CFI. Research sponsored by the Division of Materials Science and Engineering, Office of Basic Sciences, Oak Ridge National Laboratory is managed by UT-Battelle, LLC, for the U.S. Department of Energy under Contract No. DE-AC-05-00OR22725.

[1] Y. Kamihara, T. Watanabe, M. Hirano, and H. Hosono, J. Am. Chem. Soc. **130**, 3296 (2008).
[2] Z. A. Ren, W. Lu, J. Yang, W. Yi, X. L. Shen, Z. C. Li, G. C. Che, X. L. Dong, L. L. Sun, F. Zhou, and Z. X. Zhao, Chin. Phys. Lett. **25**, 2215 (2008).
[3] M. Rotter, M. Tegel, and D. Johrendt, Phys. Rev. Lett. **101**, 107006 (2008).
[4] A. S. Sefat, R. Jin, M. A. McGuire, B. C. Sales, D. J. Singh, and D. Mandrus, Phys. Rev. Lett. **101**, 117004 (2008).
[5] Y. Fukuzumi, K. Mizuhashi, K. Takenaka, and S. Uchida, Phys. Rev. Lett. **76**, 684 (1996).
[6] L. J. Li, Y. K. Luo, Q. B. Wang, H. Chen, Z. Ren, Q. Tao, Y. K. Li, X. Lin, M. He, Z. W. Zhu, G. H. Cao, and Z. A. Xu, N. J. Phys. **11**, 025008 (2009).
[7] M. Rotter, M. Tegel, I. Schellenberg, W. Hermes, R. Pottgen, and D. Johrendt, Phys. Rev. B **78**, 020503(R) (2008).
[8] Q. Huang, Y. Qiu, W. Bao, M. A. Green, J. W. Lynn, Y. C. Gasparovic, T. Wu, G. Wu, and X. H. Chen, Phys. Rev. Lett. **101**, 257003 (2008).
[9] K. Kitagawa, N. Katayama, K. Ohgushi, M. Yoshida, and M. Takigawa, J. Phys. Soc. Jpn. **77**, 114709 (2008).
[10] H. Fukazawa, K. Hirayama, K. Kondo, T. Yamazaki, Y. Kohori, N. Takeshita, K. Miyazawa, H. Kito, H. Eisaki, and A. Iyo, J. Phys. Soc. Jpn. **77**, 093706 (2008).
[11] K. Ahilan, J. Balasubramaniam, F. L. Ning, T. Imai, A. S. Sefat, R. Jin, M. A. McGuire, B. C. Sales, and D. Mandrus, J. Phys.: Condens. Matter **20**, 472201 (2008).
[12] F. L. Ning, K. Ahilan, T. Imai, A. S. Sefat, R. Jin, M. A. McGuire, B. C. Sales, and D. Mandrus, J. Phys. Soc. Jpn. **78**, 013711 (2009).
[13] N. Ni, M. E. Tillman, J. Q. Yan, A. Kracher, S. T. Hannahs, S. L. Bud'ko, and P. C. Canfield, Phys. Rev. B **78**, 214515 (2008).
[14] J. H. Chu, J. G. Analytis, C. Kucharczyk, and I. R. Fisher, Phys. Rev. B **79**, 014506 (2009).
[15] X. F. Wang, T. Wu, J. Wu, R. H. Liu, H. Chen, Y. L. Xie, and X. H. Chen, arXiv:0811.2920 (unpublished).
[16] F. C. Chou, F. Borsa, J. H. Cho, D. C. Johnston, A. Lascialfari, D. R. Torgeson, and J. Ziolo, Phys. Rev. Lett. **71**, 2323 (1993).
[17] J. H. Cho, F. Borsa, D. C. Johnston, and D. R. Torgeson, Phys. Rev. B **46**, 3179 (1992).
[18] F. L. Ning, K. Ahilan, T. Imai, A. S. Sefat, R. Jin, M. A. McGuire, B. C. Sales, and D. Mandrus, J. Phys. Soc. Jpn. **77**, 103705 (2008).
[19] H. Mukuda, N. Terasaki, H. Kinouchi, M. Yashima, Y. Kitaoka, S. Suzuki, S. Miyasaka, S. Tajima, K. Miyazawa, P. Shirage, H. Kito, H. Eisaki, and A. Iyo, J. Phys. Soc. Jpn. **77**, 093704 (2008).
[20] D. J. Singh, Phys. Rev. B **78**, 094511 (2008).
[21] Y. Nakai, K. Ishida, Y. Kamihara, M. Hirano, and H. Hosono, J. Phys. Soc. Jpn. **77**, 073701 (2008).
[22] C. Bernhard, A. J. Drew, L. Schulz, V. K. Malik, M. Rössle, Ch. Niedermayer, Th. Wolf, G. D. Varma, G. Mu, H.-H. Wen, H. Liu, G. Wu, and X. H. Chen, arXiv:0902.0859 (unpublished).